A theory of two-stream instability in two hollow relativistic electron beams

Han S. Uhm

Citation: Physics of Fluids B **5**, 3388 (1993); doi: 10.1063/1.860632
View online: http://dx.doi.org/10.1063/1.860632
View Table of Contents: http://scitation.aip.org/content/aip/journal/pofb/5/9?ver=pdfcov
Published by the AIP Publishing

Articles you may be interested in

Influence of electromagnetic effects on the two-stream instability in a relativistic electron beam
Phys. Plasmas **6**, 2636 (1999); 10.1063/1.873540

Nonlinear analysis of the two-stream instability for relativistic annular electron beams
Phys. Fluids B **5**, 4180 (1993); 10.1063/1.860963

Two-stream instability in a self-pinched relativistic electron beam
J. Appl. Phys. **56**, 2041 (1984); 10.1063/1.334248

Energy lost by a relativistic electron beam due to two-stream instability
Phys. Fluids **19**, 305 (1976); 10.1063/1.861441

Plasma heating by relativistic electron beams. I. Two-stream instability
Phys. Fluids **18**, 1552 (1975); 10.1063/1.861053

This article is copyrighted as indicated in the article. Reuse of AIP content is subject to the terms at: http://scitationnew.aip.org/termsconditions. Downloaded to IP: 35.8.11.3 On: Sun, 24 Jan 2016 23:28:00

A theory of two-stream instability in two hollow relativistic electron beams

Han S. Uhm
Naval Surface Warfare Center, 10901 New Hampshire Ave., White Oak, Silver Spring, Maryland 20903-5640

(Received 30 November 1992; accepted 7 May 1993)

Stability properties of two-stream instability of two hollow electron beams are investigated. The equilibrium configuration consists of two intense relativistic hollow electron beams propagating through a grounded conducting cylinder. Analysis of the longitudinal two-stream instability is carried out within the framework of the linearized Vlasov–Maxwell equations for the equilibrium distribution function, in which beam electrons have a Lorentzian distribution in the axial momentum. Dispersion relation of the longitudinal two-stream instability is derived. Stability criteria from this dispersion relation indicate that the normalized velocity difference $\Delta\beta$ between the beams should be within a certain range of value to be unstable. Growth rate of the instability is a substantial fraction of the real frequency, thereby indicating that the longitudinal two-stream instability is an effective means of beam current modulation. Transverse instability of hollow electron beams is also investigated. Dispersion relation of the coupled transverse oscillation of the beams is derived and numerical investigation of this dispersion relation is carried out. Growth rate of the kink instability is a substantial fraction of the diocotron frequency, which may pose a serious threat to the two-stream klystron.

I. INTRODUCTION

There is a strong renewed interest[1–5] in theoretical and experimental studies of relativistic klystron amplifiers, which generate or amplify high-power microwave radiation. Efficiency of the relativistic klystron amplifiers is determined by level of current modulation of an intense electron beam, which drives the klystron. When a beam segment passes through the opening of a microwave cavity, it gains or loses energy, depending on the sign of the cavity gap voltage. This one-time energy gain (or loss) in a single cavity klystron increases (or decreases) this beam segment velocity, modulating beam current in the downstream region. The current modulation developed in the downstream in turn generates a self-electric field, which initiates to prevent further modulation of the beam. Amplitude of the current modulation increases at the beginning and reaches a peak when influence of the initial energy modulation is balanced by that of the self-electric field due to the modulation itself.[5] Therefore, a level of the current modulation can be significantly enhanced by eliminating or reducing the influence of the self-electric field caused by the modulation. In this regard, the two-stream klystron has been proposed by the author at an engineering problems and solutions workshop[6] to enhance the current modulation, thereby improving performance of the relativistic klystron amplifiers. In the two-stream klystron amplifier, two hollow electron beams propagate in the downstream region. A charge bunching of one beam compensates for that of other beam, considerably reducing the influence of the self-electric field arising from this bunching. In addition, the self-growing mechanism of the charge bunching due to the two-stream instability of the two beams enhances further current modulation. Chen *et al.* have demonstrated the feasibility of the two-stream klystron in recent calculations.[7] In the late 1940s, the two-stream amplifier was proposed by Pierce and Hebenstreit,[8,9] and the experimental investigation of the amplifier was carried out by Hollenberg[10] and Haeff.[11] Due to inefficient input and output coupling of slow wave structures, the two-stream amplifier yielded poor efficiency. Unlike the two-stream amplifier, we expect a strong input and output coupling in resonance cavities of the two-stream klystron. However, the previous studies[8–11] demonstrated amplification of the space-charge waves in the two electron beams.

Meanwhile, Serlin and Friedman[12] have carried out the first experiment of the two-beam klystron, in which the first and second cavities communicate each other through the forward and backward beam currents, thereby exciting the first cavity to a very high level. Unlike the two-stream klystron, the two-beam klystron does not require the two-stream instability, but it needs a return current. The two-stream klystron is subjected to various physical phenomena, including influence of the axial momentum spread on the longitudinal two-stream instability and effects of the transverse two-stream instability on beam propagation. Thus, in this paper, we investigate the stability properties of the two-stream instability of hollow relativistic electron beams. The two-stream instability is also an interesting subject for the basic study of charged particle beams. The theoretical analysis in this paper is on relativistic beams with complete Maxwell's equations rather than nonrelativistic beams with Poisson's equation, as in earlier studies.[8–11]

In Sec. II, stability properties of the longitudinal two-stream instability of hollow electron beams are investigated. The stability analysis in Sec. II is carried out within the framework of the linearized Vlasov–Maxwell equations for the choice of equilibrium distribution function, in which the beam electrons have the same values of the energy and canonical angular momentum, but have a Lorentzian distribution in the axial canonical momentum. This Lorentzian distribution in the axial momentum introduces

 0899-8221/93/5(9)/3388/11/$6.00 © 1993 American Institute of Physics

This article is copyrighted as indicated in the article. Reuse of AIP content is subject to the terms at: http://scitationnew.aip.org/termsconditions. Downloaded to IP: 35.8.11.3 On: Sun, 24 Jan 2016 23:28:00

the axial momentum spread into the stability analysis. Dispersion relation of the longitudinal two-stream instability is obtained, including influence of the axial momentum spread. Stability criterion of the longitudinal two-stream instability is derived for the case of zero axial momentum spread. The necessary condition [Eq. (35)],

$$1-(1-g)^{1/2}<2\xi^2\,\Delta\beta^2/(\epsilon_1^{1/3}+\epsilon_2^{1/3})^3 < 1+(1-g)^{1/2},$$

of the longitudinal two-stream instability, is obtained for $0.02<\epsilon_1/\epsilon_2<50$. In Eq. (35), ϵ_1 and ϵ_2 are the coupling constants of the beams defined in Eqs. (20), $g=\ln(R_2/R_1)/\ln(R_c/R_1)$ is the geometrical factor of the beams, $\Delta\beta\, c$ is the velocity difference between the beams, and ξ is the electromagnetic stability factor defined in Eq. (29). Obviously, from Eq. (35), the normalized velocity difference $\Delta\beta$ should be within a certain range of value to be unstable. A few examples of beam parameters for two-stream klystrons are presented. The Massachusetts Institute of Technology (MIT) beams proposed by Chen *et al.*[7] exhibit the longitudinal two-stream instability, whereas the stability criterion in Eq. (35) predicts stability for the beams produced experimentally by Serlin and Friedman.[12] This prediction is consistent with experimental observation. Growth rate of the longitudinal two-stream instability is analytically calculated for a few limiting cases. The growth rate of instability can be a substantial fraction of the real frequency, indicating that the longitudinal two-stream instability is an effective means of beam current modulation. The axial momentum spread stabilizes the longitudinal two-stream instability effectively. For example, the normalized axial momentum spread of $\delta=0.03$ can completely stabilize the longitudinal instability for the MIT beams, wiping out the self-bunching mechanism of the two-stream klystron.

Transverse instability of hollow electron beams is investigated in Sec. III, where the two beams are assumed to be overlapping each other. The equilibrium and stability analysis in Sec. III is carried out within the framework of a macroscopic cold fluid model. Since these hollow beams have rotational velocity shear in their equilibrium, these beams exhibit instability caused by the coupled transverse oscillation and by the conventional diocotron mechanism.[13,14] The dispersion relation [Eq. (71)] for coupled transverse oscillation of two hollow electron beams is derived by making use of the linearized fluid equations. In the limit when one of the beams disappears, this dispersion relation recovers the dispersion relation of the conventional diocotron instability for a hollow electron beam. The dispersion relation [Eq. (71)] of the transverse instability is investigated numerically for a broad range of system parameters, normalizing the eigenfrequency by the diocotron frequency $\omega_D=\omega_{p2}^2/2\gamma_2^2\omega_c$ [Eq. (79)], where γ_2 is the relativistic mass ratio of electrons in the hollow beam 2, ω_{p2} is the nonrelativistic plasma frequency of the hollow beam 2, and ω_c is the nonrelativistic electron cyclotron frequency. One of the most deleterious transverse instabilities of the two hollow electron beams is the kink instability characterized by the azimuthal mode number $l=1$. It is shown from numerical calculation of the dispersion relation in Eq. (71) that the growth rate of the $l=1$ instability decreases to zero as the velocity difference $\Delta\beta$ approaches zero. This property is expected from previous studies of the diocotron instability.[13,14] For a large velocity difference between the beams, the growth rate of the $l=1$ instability is a substantial fraction of the diocotron frequency, indicating that the instability due to the coupled transverse oscillation may pose a serious threat to the two-stream klystron. The physical mechanism of instability is that one fluid element rejects the other fluid element when there is enough velocity difference between them. In order to complete the theory of the transverse instability of two hollow electron beams, we also numerically analyze the dispersion relation in Eq. (71) for high azimuthal mode numbers.

II. LONGITUDINAL TWO-STREAM INSTABILITY

The present analysis assumes that two intense annular electron beams propagate through a grounded conducting cylinder with radius R_c. The radii of the annular beams are denoted by R_1 and R_2. The inner beam radius R_1 is less than the outer beam radius R_2. The beam currents are also denoted by I_1 and I_2, respectively. A strong, externally applied magnetic field $B_0 e_z$ is needed to confine the beam electrons radially, so that the characteristic beam thicknesses are much less than the beam radii. In the theoretical analysis, we introduce a cylindrical polar coordinate system (r,θ,z). To make the analysis tractable, we assume that

$$\nu_\alpha/\gamma_\alpha \ll 1, \tag{1}$$

where $\nu_\alpha=N_\alpha e^2/mc^2$ is Budker's parameter of the beam α, $\gamma_\alpha mc^2$ is the characteristic electron energy of the beam α, c is the speed of light in vacuum, $-e$ and m are electron charge and rest mass, respectively, and N_α is the number of electrons per unit axial length of the beam α.

The stability analysis of the longitudinal two-stream instability is carried out within the framework of the linearized Vlasov–Maxwell equations, in order to investigate influence of the axial momentum spread on stability behavior. In the present analysis, we investigate stability properties of the longitudinal two-stream for the choice of equilibrium distribution function,

$$f_\alpha^0(H,P_\theta,P_z)=\frac{\omega_c N_\alpha \Delta_\alpha}{4\pi^2\gamma_\alpha mc^2}\,\frac{\delta(H/mc^2-\gamma_{\alpha m})\delta(P_\theta-P_\alpha)}{(P_z-\gamma_\alpha m\beta_\alpha c)^2+\Delta_\alpha^2}, \tag{2}$$

where

$$H=(m^2c^4+c^2p^2)^{1/2}-e\phi_0(r) \tag{3}$$

is the total energy, $P_\theta=r[p_\theta-(e/2c)rB_0]$ is the canonical angular momentum, $P_z=p_z+(e/c)A_z^0(r)$ is the axial canonical momentum, $\omega_c=eB_0/mc$ is the electron cyclotron frequency,

$$P_\alpha=-(e/2c)(R_\alpha^2-r_{L\alpha}^2)B_0 \tag{4}$$

is the canonical angular momentum of an electron with Larmor radius,

This article is copyrighted as indicated in the article. Reuse of AIP content is subject to the terms at: http://scitationnew.aip.org/termsconditions. Downloaded to IP: 35.8.11.3 On: Sun, 24 Jan 2016 23:28:00

$$r_{L\alpha}=(\gamma_\alpha c/\omega_c)[(\gamma_{\alpha m}-\gamma_\alpha)/\gamma_\alpha]^{1/2}, \tag{5}$$

for the beam α, and $\gamma_\alpha=(1-\beta_\alpha^2)^{(-1/2)}$, and Δ_α are constants. Here, $\phi_0(r)$ is the electrostatic potential for the equilibrium self-electric field and $A_z^0(r)$ is the axial component of vector potential for the azimuthal self-magnetic field. Within the context of Eq. (1), the equilibrium vector potential $A_z^0(r)$ is neglected in the analysis in this section. Note from Eq. (2) that the beam electrons have a Lorentzian distribution in the axial canonical momentum.

A. Dispersion relation of longitudinal two-stream instability

In the stability analysis, use is made of the linearized Vlasov–Maxwell equations for azimuthally symmetric perturbations ($\partial/\partial\theta=0$) about two hollow beams described by Eq. (2). We adopt a normal mode approach in which all perturbations are assumed to vary according to

$$\delta\Psi(x,t)=\Psi(r)\exp[i(kz-\omega t)], \tag{6}$$

where Im $\omega>0$. Here, ω is the complex eigenfrequency and k is the axial wave number. The Maxwell equations for the perturbed electric and magnetic field amplitudes can be expressed,

$$E_r(r)=(kc/\omega)B_\theta(r),$$
$$B_\theta(r)=i\left(\frac{\omega}{cp^2}\right)\left(\frac{\partial E_z(r)}{\partial r}\right), \tag{7}$$

and

$$\left(\frac{1}{r}\frac{\partial}{\partial r}r\frac{\partial}{\partial r}-p^2\right)E_z(r)=4\pi ik\left(\rho(r)-\frac{\omega}{c^2k}J_z(r)\right), \tag{8}$$

where B_θ is the azimuthal component of the perturbed magnetic field, E_r and E_z are the radial and axial components, respectively, of the perturbed electric field, $\rho(r)$ is the perturbed charge density, and $J_z(r)$ is the axial component of the perturbed current density. The parameter p^2 in Eq. (8) is defined by

$$p^2=k^2-\frac{\omega^2}{c^2}. \tag{9}$$

To the lowest order, the axial motion of the particle orbit is free streaming,

$$z'=z+(p_z/\gamma m)(t'-t). \tag{10}$$

Moreover, within the context of Eq. (1), we neglect the terms proportional to $E_\perp$ in the calculation of the perturbed distribution function δf_α. Here $E_\perp$ is the transverse component of the perturbed electric field. Because the oscillatory modulation of the radial orbit is small ($r_{L\alpha}\ll R_\alpha$), we make the approximation $r'=r$ in the calculation of the perturbed distribution function. Under these approximations, we carry out the characteristic time and momentum integrations, in order to find the perturbed charge and current densities. After a straightforward calculation, it is shown that Eq. (8) is expressed as

$$\left(\frac{1}{r}\frac{\partial}{\partial r}r\frac{\partial}{\partial r}-p^2\right)E_z(r)=-\sum_\alpha\frac{\delta(r-R_\alpha)}{R_\alpha}\sigma_\alpha E_z(r), \tag{11}$$

where the source function $\sigma_\alpha(\omega,k)$ is defined by

$$\sigma_\alpha(\omega,k)=\frac{2\nu_\alpha}{\gamma_\alpha^3}\frac{k^2c^2-\omega^2}{(\omega-k\beta_\alpha c+ik\Delta_\alpha/\gamma_\alpha^3 m)^2}, \tag{12}$$

and the Budker's parameter ν_α is related to the beam current by

$$\nu_\alpha=\frac{eI_\alpha}{m\beta_\alpha c^3}. \tag{13}$$

For a detailed derivation of Eq. (11), we recommend that readers review the previous literature.[11]

For the present purposes, the stability analysis is restricted to the long-wavelength perturbation, characterized by

$$k^2R_\alpha^2\ll\gamma_\alpha^2, \tag{14}$$

which is common in many two-stream applications. The eigenvalue equation (11) for the long-wavelength perturbations is simplified to

$$\frac{1}{r}\frac{\partial}{\partial r}r\frac{\partial}{\partial r}E_z(r)=-\sum_\alpha\frac{\delta(r-R_\alpha)}{R_\alpha}\sigma_\alpha(\omega,k)E_z(r). \tag{15}$$

The physically acceptable solution to Eq. (15) is

$$E_z(r)=\begin{cases}E_{\rm I}(r)=A, & 0<r<R_1,\\ E_{\rm II}(r)=B+C\ln(r), & R_1<r<R_2,\\ E_{\rm III}(r)=D\ln(R_c/r), & R_2<r<R_c,\end{cases} \tag{16}$$

where A, B, C, and D are constants. Multiplying both sides of Eq. (15) by r and integrating in the radial coordinate across $r=R_1$, we have

$$\left(\frac{\partial E_{\rm I}}{\partial r}\right)_{R_1}-\left(\frac{\partial E_{\rm II}}{\partial r}\right)_{R_1}=\sigma_1(\omega,k)\frac{E_z(R_1)}{R_1}. \tag{17}$$

Similarly, we also obtain

$$\left(\frac{\partial E_{\rm II}}{\partial r}\right)_{R_2}-\left(\frac{\partial E_{\rm III}}{\partial r}\right)_{R_2}=\sigma_2(\omega,k)\frac{E_z(R_2)}{R_2}. \tag{18}$$

Substituting Eq. (16) into Eqs. (17) and (18), and making use of the continuity property of the axial electric field at $r=R_1$ and $r=R_2$, we obtain the dispersion relation,

$$\sigma_1\ln\left(\frac{R_c}{R_1}\right)+\sigma_2\ln\left(\frac{R_c}{R_2}\right)-\sigma_1\sigma_2\ln\left(\frac{R_2}{R_1}\right)\ln\left(\frac{R_c}{R_2}\right)=1. \tag{19}$$

For convenience in the subsequent analysis, we introduce the parameter ϵ_α, defined by

$$\epsilon_\alpha=\frac{2}{\gamma_\alpha^3\beta_\alpha}\frac{I_\alpha}{I_{\rm A}}\ln\left(\frac{R_c}{R_\alpha}\right), \tag{20}$$

where $I_{\rm A}=mc^3/e=17$ kA is the Alfvén current. Substituting Eq. (12) into Eq. (19) and making use of the definition of ϵ_α in Eq. (20), it can be shown that the dispersion relation in Eq. (19) is expressed as

This article is copyrighted as indicated in the article. Reuse of AIP content is subject to the terms at: http://scitationnew.aip.org/termsconditions. Downloaded to IP: 35.8.11.3 On: Sun, 24 Jan 2016 23:28:00

$$0=1-\sum_{\alpha=1}^{2}\frac{\epsilon_\alpha(c^2k^2-\omega^2)}{(\omega-k\beta_\alpha c+ik\Delta_\alpha/\gamma_\alpha^3 m)^2}+\frac{\ln(R_2/R_1)}{\ln(R_c/R_1)}\frac{\epsilon_1\epsilon_2(c^2k^2-\omega^2)^2}{(\omega-k\beta_1 c+ik\Delta_1/\gamma_1^3 m)^2(\omega-k\beta_2 c+ik\Delta_2/\gamma_2^3 m)^2}, \tag{21}$$

which can be used to investigate stability properties of the longitudinal two-stream instability for a broad range of system parameters. In the limit of no axial momentum spread ($\Delta_1=\Delta_2=0$), the dispersion relation in Eq. (21) recovers the previous result obtained by Chen *et al.*[7]

B. Stability criterion of longitudinal two-stream instability

The stability criterion in this section is derived for the case of zero axial momentum spread characterized by $\Delta_\alpha=0$. Assuming that the two beams are located very close, we can neglect the last stabilizing term in Eq. (21) and the dispersion relation of the instability for overlapping beams is given by

$$1=\frac{\epsilon_1(c^2k^2-\omega^2)}{(\omega-k\beta_1 c)^2}+\frac{\epsilon_2(c^2k^2-\omega^2)}{(\omega-k\beta_2 c)^2}. \tag{22}$$

Without loss of generality, we assume $\beta_2>\beta_1$. Defining the Doppler-shifted frequency,

$$\Omega=\omega-k\beta_1 c, \tag{23}$$

and the velocity difference $\Delta\beta=\beta_2-\beta_1$, Eq. (22) is expressed as

$$1=\frac{\epsilon_1 p^2c^2}{\Omega^2}+\frac{\epsilon_2 p^2c^2}{(\Omega-k\,\Delta\beta\, c)^2}, \tag{24}$$

where $p^2=k^2-\omega^2/c^2$ is defined in Eq. (9). The local minimum point of the right-hand side of Eq. (24) occurs at[16,17]

$$\Omega=\Omega_p=k\,\Delta\beta\, c\,\frac{\eta}{1+\eta}, \tag{25}$$

where the parameter

$$\eta=(\epsilon_1/\epsilon_2)^{1/3} \tag{26}$$

represents the ratio of the coupling strength of the two-stream instability. In obtaining Eq. (25), we have neglected the effects arising from dependence of the parameter p^2 in Eq. (24) on the frequency ω in the range of $k\beta_1 c<\omega<k\beta_2 c$. These effects on stability properties are not very critical.

The instability occurs when the right-hand side of Eq. (24) at $\Omega=\Omega_p$ is larger than unity. Thus, the necessary condition for instability of the dispersion relation in Eq. (24) is given by[16,17]

$$k^2\,\Delta\beta^2<\epsilon_1 p^2[1+(\epsilon_2/\epsilon_1)^{1/3}]^3. \tag{27}$$

The phase velocity $\beta_p c$ of the unstable wave is also given by

$$\beta_p=\frac{\omega}{kc}=\beta_1+\frac{\Omega_p}{kc}=\beta_1+\Delta\beta\,\frac{\eta}{1+\eta}. \tag{28}$$

Note from Eq. (28) that the phase velocity of the unstable wave is very close to the beam velocity $\beta_1 c$ for $\epsilon_1\ll\epsilon_2$. On the other hand, $\beta_p\approx\beta_2$ for $\epsilon_2\ll\epsilon_1$. Substituting Eq. (28) into Eq. (9) and defining the electromagnetic stability factor ξ by

$$\xi^2=\frac{1}{1-\beta_p^2}=\frac{1}{1-[\beta_1+\Delta\beta\eta/(1+\eta)]^2}, \tag{29}$$

the parameter p in Eq. (9) is approximated by $p=k/\xi$. Therefore, the instability condition in Eq. (27) is expressed as

$$y^3=(\epsilon_1^{1/3}+\epsilon_2^{1/3})^3>\xi^2\,\Delta\beta^2. \tag{30}$$

Note from Eq. (29) that the electromagnetic stability factor ξ is almost linearly proportional to the relativistic mass ratio γ of the beams.

When the beams are located at different locations ($R_1\neq R_2$), the dispersion relation for $\Delta_\alpha=0$ is given by

$$1=\sum_{\alpha=1}^{2}\frac{\epsilon_\alpha(c^2k^2-\omega^2)}{(\omega-k\beta_\alpha c)^2}-\frac{\ln(R_2/R_1)}{\ln(R_c/R_1)}\frac{\epsilon_1\epsilon_2(c^2k^2-\omega^2)^2}{(\omega-k\beta_1 c)^2(\omega-k\beta_2 c)^2}, \tag{31}$$

from Eq. (21). For convenience in the subsequent analysis, we define the geometrical factor g by

$$g=\frac{\ln(R_2/R_1)}{\ln(R_c/R_1)}, \tag{32}$$

which is always less than unity. For relativistic electron beams satisfying $g\ll\xi^2$, we can show that the local minimum of the right-hand side of Eq. (31) occurs at the frequency $\omega=\beta_p kc$. Here, the phase velocity $\beta_p c$ is defined in Eq. (28). The instability occurs when the right-hand side of Eq. (31) at the frequency $\omega=k\beta_p c$ is larger than unity. Therefore, after a straightforward calculation, we obtain the necessary condition

$$y^3>\xi^2\,\Delta\beta^2+g\,\frac{(\epsilon_1\epsilon_2)^{1/3}}{\xi^2\,\Delta\beta^2}\,y^4, \tag{33}$$

for instability, when the two beams have different radii. Making use of the definition η in Eq. (26), the instability criterion in Eq. (33) is equivalently expressed as

$$1-\sqrt{1-4g\,\frac{\eta}{(1+\eta)^2}}<\frac{2\xi^2\,\Delta\beta^2}{y^3}<1+\sqrt{1-4g\,\frac{\eta}{(1+\eta)^2}}, \tag{34}$$

for $R_1\neq R_2$. We remind the reader that the criterion in Eq. (34) is valid only for relativistic beams satisfying $g\ll\xi^2$. The factor $\eta/(1+\eta)^2$ in Eq. (34) decreases from unity to zero, as the current ratio ϵ_1/ϵ_2 increases from unity to infinity or decreases from unity to zero. However, this fac-

This article is copyrighted as indicated in the article. Reuse of AIP content is subject to the terms at: http://scitationnew.aip.org/termsconditions. Downloaded to IP: 35.8.11.3 On: Sun, 24 Jan 2016 23:28:00

TABLE I. A few examples of the two-stream kylstron amplifiers. The upper and lower bounds in the table represent the instability boundary in Eq. (34).

	MIT beams[a]	NRL beams[b]	Sample beams
R_c (cm)	2.54	2.35	2.5
R_1 (cm)	2.08	1.4	1.5
R_2 (cm)	2.29	2	2.25
I_1 (kA)	1	3	7
I_2 (kA)	5	9	1
γ_1 (γ_{01})	1.32 (1.43)	1.78 (2.2)	1.3 (2)
γ_2 (γ_{02})	1.69 (1.78)	1.93 (2.2)	1.83 (2)
η	1	1.1	5
g	0.48	0.69	0.79
Upper bound	1.72	1.56	1.75
$2\xi^2\,\Delta\beta^2/y^3$	0.8	0.023	0.4
Lower bound	0.28	0.44	0.25
	unstable	stable	marginal

[a]C. Chen, P. Catravas, and G. Bekefi, Appl. Phys. Lett. **62**, 1579 (1993).
[b]V. Serlin and M. Friedman, Appl. Phys. Lett. **62**, 2772 (1993).

tor has the maximum value of unity at $\eta=1$ and decreases slowly as the parameter η deviates from unity. Therefore, the inequality in Eq. (34) is simplified to

$$1-\sqrt{1-g}<\frac{2\xi^2\,\Delta\beta^2}{y^3}<1+\sqrt{1-g}, \tag{35}$$

for the current ratio, satisfying $0.02<\epsilon_1/\epsilon_2<50$, which is case in most of the present experimental applications. Note from Eqs. (32) and (35) that there is no unstable region when the outer beam approaches the cylindrical conductor ($R_2\to R_c$).

Presented in Table I are a few examples of the two-stream klystron amplifiers. Chen *et al.*[7] at the Massachusetts Institute of Technology (MIT) have proposed the two-stream klystron amplifier by making use of the beams, which are injected from two different cathodes. The injection energies of beams 1 and 2 are $\gamma_{01}=1.43$ and $\gamma_{02}=1.78$, respectively. Undoubtedly, these beams must be injected from two different accelerators. The beam energies in the waveguide are less than the injection energies, due to the self-potential depression. The beam energies γ_1 and γ_2 are calculated from

$$\begin{aligned}\gamma_1&=\gamma_{01}-\frac{2eI_1}{m\beta_1c^3}\ln\left(\frac{R_c}{R_1}\right)-\frac{2eI_2}{m\beta_2c^3}\ln\left(\frac{R_c}{R_2}\right),\\ \gamma_2&=\gamma_{02}-\left(\frac{2eI_1}{m\beta_1c^3}+\frac{2eI_2}{m\beta_2c^3}\right)\ln\left(\frac{R_c}{R_2}\right),\end{aligned} \tag{36}$$

for specified injection energies γ_{01} and γ_{02} of the beams. Because the two MIT beams have an enough energy difference (or velocity difference), value of the parameter $2\xi^2\,\Delta\beta^2/y^3$ in Eq. (34) is comfortably inside the instability boundary, as shown in Table I. Therefore, the MIT beams are useful for the two-stream klystron amplifier.

Serlin and Friedman[12] at the Naval Research Laboratory (NRL) have conducted a two beam klystron experiment, in which the beams are injected into the klystron from a single cathode. As shown in Table I, the injection energy of these beams is $\gamma_{01}=\gamma_{02}=2.2$. According to Eq. (36), the energies of the inner and outer beams in the klystron are given by $\gamma_1=1.78$ and $\gamma_2=1.93$, respectively, for $I_1=3$ kA and $I_2=9$ kA. In these physical parameter ranges, the velocity difference between the inner and outer beams is $\Delta\beta=0.0283$, which is too small to initiate the two-stream instability. Note from Table I that the parameter $2\xi^2\,\Delta\beta^2/y^3=0.023$ is much less than the lower boundary, $1-(1-g)^{1/2}=0.44$, for instability. Thus we predict stability for Naval Research Laboratory (NRL) beams, which is consistent with experimental observations made by Friedman and Serlin in 1992. The sample beams in the last columns are injected from a single cathode, with inner and outer radii of $R_1=1.5$ cm and $R_2=2.25$ cm. The injection energy is $\gamma_{01}=\gamma_{02}=2$. Energies of the inner and outer beams are $\gamma_1=1.3$ and $\gamma_2=1.83$, respectively, for $I_1=7$ kA and $I_2=1$ kA, according to Eq. (36). Note from Table I that the inner current is larger than the outer current. In the sample beam parameters, the velocity difference between the inner and outer beams is $\Delta\beta=0.2$, generating a relatively large value of the parameter $2\xi^2\,\Delta\beta^2/y^3=0.4$ and ensuring a marginal instability. However, the growth rate of instability may not be large. Even beams injected from a same cathode can be unstable in appropriate physical parameters, as shown in these examples. There may be a certain range of beam paramcters, which ensure both the beam propagation and instability for beams injected from a single cathode. Growth rate of the longitudinal two-stream instability should also be a substantial fraction of the frequency, to be useful for the two-stream klystron. Beam propagation and stability behavior for single-cathode beams are currently under investigation by the author, and will be presented elsewhere.

C. Growth rate of longitudinal two-stream instability

An investigation of the dispersion relation in Eq. (21) is not analytically tractable, in general. Thus, in this section, the stability analysis is restricted to the case of zero axial momentum spread. In addition, we also concentrated on the special cases of $\epsilon_1\simeq\epsilon_2$, $\epsilon_2/\epsilon_1\ll1$, and $\epsilon_1/\epsilon_2\ll1$.

For the case when $\epsilon_1=\epsilon_2=\epsilon$, the dispersion relation in Eq. (31) is expressed as

$$\frac{2\epsilon(x^2+\Delta\beta^2/4)/\xi^2}{(x^2-\Delta\beta^2/4)^2}=1+g\,\frac{\epsilon^2/\xi^4}{(x^2-\Delta\beta^2/4)^2}, \tag{37}$$

where the normalized Doppler-shifted frequency x is defined by

$$x=\frac{\omega-k(\beta_1+\beta_2)/2}{kc}, \tag{38}$$

and the normalized velocity difference is $\Delta\beta=\beta_2-\beta_1$. After carrying out a straightforward calculation, the solution of Eq. (37) is expressed as

$$x^2=\frac{\epsilon}{\xi^2}+\frac{\Delta\beta^2}{4}-\sqrt{(1-g)\,\frac{\epsilon^2}{\xi^4}+\frac{\epsilon\,\Delta\beta^2}{\xi^2}}, \tag{39}$$

This article is copyrighted as indicated in the article. Reuse of AIP content is subject to the terms at: http://scitationnew.aip.org/termsconditions. Downloaded to IP: 35.8.11.3 On: Sun, 24 Jan 2016 23:28:00

where the electromagnetic stability factor ξ is defined in Eq. (29). The necessary condition for instability found from Eq. (39) is identical to Eq. (35) for $y=8\epsilon$. The normalized maximum growth rate,

$$x_i=\frac{\sqrt{1-g}}{2}\frac{\sqrt{\epsilon}}{\xi}, \tag{40}$$

of the instability occurs at the velocity difference, satisfying

$$\Delta\beta^2=(3+g)\frac{\epsilon}{\xi^2}. \tag{41}$$

For the case when $\epsilon_1 \gg \epsilon_2$, the local minimum point of the right-hand side of Eq. (31) occurs near $\omega=k\beta_2 c$, and Eq. (31) is approximated by

$$x^3+\frac{1}{2}\left(\Delta\beta-\frac{\epsilon_1}{\Delta\beta\,\xi^2}\right)x^2-\frac{\epsilon_2}{\xi^2}x-\frac{\epsilon_2}{2\xi^2}\left(\Delta\beta-g\frac{\epsilon_1}{\Delta\beta\,\xi^2}\right)=0, \tag{42}$$

where the Doppler-shifted frequency x is defined by $x=(\omega-k\beta_2 c)/kc$. After a careful examination of solutions of cubic equations, we can show that the maximum growth rate of Eq. (42) occurs the velocity difference, such that

$$\Delta\beta\approx\frac{\sqrt{\epsilon_1}}{\xi}. \tag{43}$$

Substituting Eq. (43) into Eq. (42), the dispersion relation in Eq. (42) can be solved for maximum growth, eventually yielding

$$x_i=\mathrm{Im}(x)=\frac{\sqrt{3}}{2\xi}\left(\frac{\epsilon_2\sqrt{\epsilon_1}}{2}(1-g)\right)^{1/3}. \tag{44}$$

For the case of $\epsilon_1 \ll \epsilon_2$, the dispersion relation in Eq. (31) can be approximated by

$$x^3-\frac{1}{2}\left(\Delta\beta-\frac{\epsilon_2}{\Delta\beta\,\xi^2}\right)x^2-\frac{\epsilon_1}{\xi^2}x+\frac{\epsilon_1}{2\xi^2}\left(\Delta\beta-g\frac{\epsilon_1}{\Delta\beta\,\xi^2}\right)=0, \tag{45}$$

where $x=(\omega-k\beta_1 c)/kc$. The solution of Eq. (45) for the maximum growth rate is

$$x=\frac{1}{2\xi}(1\pm i\sqrt{3})\left(\frac{\epsilon_1\sqrt{\epsilon_2}}{2}(1-g)\right)^{1/3}, \tag{46}$$

which occurs at the velocity difference $\Delta\beta\approx\epsilon_2^{1/2}/\xi$. A rough estimation of the growth rates for instability can be obtained from Eqs. (40), (44), and (46). In any event, the growth rate of the longitudinal two-stream instability can be a substantial fraction of the real frequency. For additional information of the instability, we urge the reader to numerically evaluate the growth rate from Eq. (31).

D. Influence of the axial momentum spread on stability properties

Analysis of the dispersion relation in Eq. (21) is very complicated in general. However, in the limited case when

$$\frac{\Delta_1}{\gamma_1^3 mc}=\frac{\Delta_2}{\gamma_2^3 mc}=\delta, \tag{47}$$

the normalized Doppler-shifted frequency x in Eqs. (37), (42), and (45) can include the spread δ. For example, for $\epsilon_1=\epsilon_2=\epsilon$, Doppler-shifted frequency x can be defined by $x=(\omega/kc)-(\beta_1+\beta_2)/2+i\delta$, and the normalized growth rate x_i has been calculated in Eq. (40). Therefore, the maximum growth rate $\omega_i=\mathrm{Im}\,\omega$ of the instability is expressed as

$$\omega_i=\left(\frac{\sqrt{1-g}}{2}\frac{\sqrt{\epsilon}}{\xi}-\delta\right)kc, \tag{48}$$

which requires a very small axial momentum spread to assure instability. The normalized momentum spread δ should be less than three percent for MIT beams[7] to be unstable. The threshold momentum spread of instability is $\delta_{\mathrm{th}}=[(1-g)\epsilon]^{1/2}/2\xi$ from Eq. (48) for $\epsilon_1=\epsilon_2=\epsilon$. Because the maximum growth rate in Eq. (48) has been obtained for the optimum velocity difference in Eq. (41), we find the inequality $2\delta/\Delta\beta<[(1-g)/(3+g)]^{1/2}$ to assure the instability. For MIT beams with $g=0.48$, the instability criterion is given by $2\delta/\Delta\beta<0.39$, which may not be difficult to satisfy. However, any value of the momentum spread reduces growth rate drastically, as shown in Eq. (48).

Eliminating or reducing the axial momentum spread is pivotally important in the two-stream klystron. The momentum spread originates from several physical phenomena. Because the annual beams have finite thickness, the axial momenta at inner and outer surfaces of the beam have different values. Assuming that radii of the inner and outer surfaces of the beam are denoted by a and b, the momentum spread Δ_2 of the beam 2 is estimated by

$$\frac{\Delta_2}{\gamma_2 m\beta_2 c}=\frac{I_1+I_2}{2I_A\gamma_2\beta_2}\ln\left(\frac{b}{a}\right), \tag{49}$$

which is proportional to the beam thickness of $b-a$. The thinner the beam thickness the lesser the axial momentum spread due to the self-potential depression. However, as will be seen in the next section [Eq. (78)], the diocotron frequency of a specified beam intensity increases as the beam thickness decreases. Meanwhile, instability due to the transverse perturbations increases as the diocotron frequency increases. The transverse temperature of the beam also causes the axial momentum spread.

III. TRANSVERSE INSTABILITY OF HOLLOW ELECTRON BEAMS

In this section, we study properties of the transverse two-stream instability, assuming that the two hollow beams are overlapping each other. The transverse two-stream instability is initially caused by a misalignment of the beams. Even if there is a relatively strong growth of the transverse two-stream instability, a proper control of any misalignment of the beams and unnecessary initial perturbations may suppress the instability under an acceptable level. Thus, the stability analysis in this section is concentrated on the overlapping beams, which will provide the necessary information of the transverse two-stream instability. If needed, the analysis can be extended to nonoverlapping case in a straightforward manner.

This article is copyrighted as indicated in the article. Reuse of AIP content is subject to the terms at: http://scitationnew.aip.org/termsconditions. Downloaded to IP: 35.8.11.3 On: Sun, 24 Jan 2016 23:28:00

The equilibrium configuration consists of intense hollow electron beams that are infinite in axial extent and propagate through a cylindrical conducting wall with radius R_c. The inner and outer radii of the surface of the hollow beams are represented by a and b, respectively. The applied axial magnetic field $B_0 e_z$ provides confinement of the equilibrium configuration in the radial direction. In order to make the analysis tractable, we assume that the hollow beams are relatively tenuous, satisfying

$$\gamma_\alpha \omega_{p\alpha}^2 \ll \omega_c^2, \tag{50}$$

where ${\omega_{p\alpha}}^2 = 4\pi e^2 n_\alpha / m$ is the plasma frequency squared of hollow beam α and $\omega_c = eB_0/mc$ is the nonrelativistic electron cyclotron frequency.

The equilibrium and stability analysis in this section is carried out within the framework of a macroscopic cold fluid model. In this context, the equation of motion and the continuity equation for the hollow electron fluid can be expressed as

$$\left(\frac{\partial}{\partial t} + \mathbf{V}_\alpha \cdot \nabla\right) \gamma_\alpha m \mathbf{V}_\alpha = -e\left(\mathbf{E}_T + \frac{\mathbf{V}_\alpha x \mathbf{B}_T}{c}\right) \tag{51}$$

and

$$\frac{\partial}{\partial t} n_\alpha + \nabla \cdot (n_\alpha \mathbf{V}_\alpha) = 0, \tag{52}$$

where $\mathbf{E}_T$ and $\mathbf{B}_T$ are electric and magnetic fields, respectively, and n_α and $\mathbf{V}_\alpha$ are the density and mean velocity, respectively, of the electron fluid element in the hollow beam α. For present purposes, we also specialize to the sharp-boundary density profile of the hollow electron beams, given by

$$n_\alpha^0(r) = \begin{cases} n_\alpha = \text{const}, & a < r < b, \\ 0, & \text{otherwise.} \end{cases} \tag{53}$$

Since the mean velocity of an electron fluid element in the hollow electron beams is specified by $\mathbf{V}_\alpha^0(r) = V_{\alpha\theta}^0(r)\mathbf{e}_\theta + \beta_\alpha c \mathbf{e}_z$, the steady-state equation of motion in the azimuthal direction can be expressed as

$$\gamma_\alpha m V_{\alpha\theta}^0(r)^2 / r = e[E_r^0(r) - \beta_\alpha B_\theta^0(r) + V_{\alpha\theta}^0(r) B_0/c], \tag{54}$$

from Eq. (51). In Eqs. (54), $E_r^0(r)$ and $B_\theta^0(r)$ are the equilibrium radial electric and azimuthal magnetic fields, and $\mathbf{e}_\theta$ and $\mathbf{e}_z$ are unit vectors in the radial and azimuthal directions. Making use of the density profile in Eq. (53), it can be found that the field combination $E_r^0(r) - \beta_1 B_\theta^0(r)$ in Eq. (54) is expressed as

$$\begin{aligned} E_r^0(r) - \beta_1 B_\theta^0(r) &= -\frac{\partial}{\partial r}[\phi_0(r) - \beta_1 A_z^0(r)] \\ &= -2\pi e\left(\frac{n_1}{\gamma_1^2} + n_2(1-\beta_1\beta_2)\right)\left(r - \frac{a^2}{r}\right), \end{aligned} \tag{55}$$

for $a < r < b$. Here, $\phi_0(r)$ is the electrostatic potential for the equilibrium self-electric field and $A_z^0(r)$ is the axial component of the vector potential for the azimuthal self-magnetic field. Substituting Eq. (55) into Eq. (54), and making use of Eqs. (1) and (50), we obtain the slow rotational frequency $\omega_1(r)$,

$$\omega_1(r) = \frac{1}{2\omega_c}\left(\frac{\omega_{p1}^2}{\gamma_1^2} + \omega_{p2}^2(1-\beta_1\beta_2)\right)\left(1 - \frac{a^2}{r^2}\right), \tag{56}$$

of the hollow beam 1. Similarly, the slow rotational frequency $\omega_2(r)$ of the hollow beam 2 is obtained and expressed as

$$\omega_2(r) = \frac{1}{2\omega_c}\left(\frac{\omega_{p2}^2}{\gamma_2^2} + \omega_{p1}^2(1-\beta_1\beta_2)\right)\left(1 - \frac{a^2}{r^2}\right). \tag{57}$$

Note from Eqs. (56) and (57) that beam rotational frequencies at the inner surface of the beams ($r = a$) are zero.

A. Dispersion relation of the transverse two-stream instability

In the stability analysis of this section, we make use of the linearized fluid and Maxwell equations to obtain the dispersion relation for coupled transverse oscillation of two hollow electron beams. Again, we adopt a normal mode approach in which all perturbations are assumed to vary with time and space according to

$$\delta\Psi(x,t) = \Psi(r)\exp[i(l\theta + kz - \omega t)], \tag{58}$$

where l is the azimuthal harmonic number and k is the axial wave number. The analysis in the section is also carried out for long axial wavelength perturbations, satisfying

$$k^2 R_c^2 \ll (l^2+1). \tag{59}$$

Moreover, the stability properties are investigated for low-frequency perturbations, satisfying

$$\omega^2 R_c^2 \ll (l^2+1). \tag{60}$$

Within the context of Eqs. (59) and (60), it is straightforward to show that the Maxwell equations for perturbed fields can be approximated by

$$\left(\frac{1}{r}\frac{\partial}{\partial r} r \frac{\partial}{\partial r} - \frac{l^2}{r^2}\right)\phi(r) = -4\pi\rho(r) \tag{61}$$

and

$$\left(\frac{1}{r}\frac{\partial}{\partial r} r \frac{\partial}{\partial r} - \frac{l^2}{r^2}\right)A(r) = -\frac{4\pi}{c} J(r), \tag{62}$$

where $\phi(r)$ and $\rho(r)$ are the perturbed electric potential and charge density, respectively, and $A(r)$ and $J(r)$ are the axial components of the perturbed vector potential and current density, respectively. Components of the perturbed fields can be expressed in terms of $\phi(r)$ and $A(r)$ as

$$\begin{aligned} &E_r(r) = -\left(\frac{\partial}{\partial r}\right)\phi(r), \quad E_\theta(r) = -\left(\frac{il}{r}\right)\phi(r), \\ &E_\theta(r) = -\left(\frac{\partial}{\partial r}\right)A(r), \quad B_r(r) = \left(\frac{il}{r}\right)A(r). \end{aligned} \tag{63}$$

The perturbed charge $\rho_\alpha(r)$ and current $J_\alpha(r)$ densities contributed by the hollow beam α can be calculated by

This article is copyrighted as indicated in the article. Reuse of AIP content is subject to the terms at: http://scitationnew.aip.org/termsconditions. Downloaded to IP: 35.8.11.3 On: Sun, 24 Jan 2016 23:28:00

linearizing the macroscopic fluid descriptions in Eqs. (51) and (52). Defining the effective perturbed potential

$$\Phi_\alpha(r)=\phi(r)-\beta_\alpha A(r), \tag{64}$$

and carrying out a straightforward algebraic manipulation, we obtain the perturbed charge density,[13]

$$\rho_\alpha(r)=J_\alpha(r)/\beta_\alpha c$$
$$=\frac{l\Phi_\alpha(r)}{4\pi r}\frac{1}{\omega_c[\omega-k\beta_\alpha c-l\omega_\alpha(r)]}\frac{\partial}{\partial r}\omega_{p\alpha}^2(r), \tag{65}$$

contributed by the hollow beam α. In Eq. (65), $\omega_{p\alpha}{}^2(r)=4\pi e n_\alpha{}^0(r)/m$ is the nonrelativistic plasma frequency squared of the hollow beam α and its derivative $(\partial/\partial r)\omega_{p\alpha}{}^2(r)$ can be expressed as

$$\frac{\partial}{\partial r}\omega_{p\alpha}^2(r)=\omega_{p\alpha}^2[\delta(r-a)-\delta(r-b)], \tag{66}$$

from Eq. (53).

Substituting Eq. (65) into Eqs. (61) and (62), and making use of the definition of the effective perturbed potential $\Phi_\alpha(r)$ in Eq. (64), give the coupled eigenvalue equations,

$$\left(\frac{1}{r}\frac{\partial}{\partial r}r\frac{\partial}{\partial r}-\frac{l^2}{r^2}\right)\Phi_1(r)$$
$$=-\frac{l}{r}\left(\Phi_1(r)\frac{H_1(r)}{\gamma_1^2}+\Phi_2(r)H_2(r)(1-\beta_1\beta_2)\right)$$
$$\times[\delta(r-a)-\delta(r-b)] \tag{67}$$

and

$$\left(\frac{1}{r}\frac{\partial}{\partial r}r\frac{\partial}{\partial r}-\frac{l^2}{r^2}\right)\Phi_2(r)$$
$$=-\frac{l}{r}\left(\Phi_1(r)H_1(r)(1-\beta_1\beta_2)+\Phi_2(r)\frac{H_2(r)}{\gamma_2^2}\right)$$
$$\times[\delta(r-a)-\delta(r-b)], \tag{68}$$

where the effective susceptibility of the hollow electron beam α is defined by

$$H_\alpha(r)=\frac{\omega_{p\alpha}^2}{\omega_c[\omega-k\beta_\alpha-l\omega_\alpha(r)]}. \tag{69}$$

It is evident that the right-hand side of Eqs. (67) and (68) are equal to zero except at the surface of the beam boundaries ($r=a$ and $r=b$). Therefore, the eigenvalue equations in Eqs. (67) and (68) can be reduced to $r^{-1}(\partial/\partial r)(\partial\Phi_\alpha/\partial r)-(l^2/r^2)\Phi_\alpha=0$, except $r=a$ and $r=b$. The eigenfunction satisfying Eqs. (67) and (68) are expressed as

$$\Phi_\alpha(r)=\begin{cases}B_\alpha r^l+C_\alpha a^{-2l}r^l, & 0<r<a,\\ B_\alpha r^l+C_\alpha r^{-l} & a<r<b,\\ (B_\alpha b^{2l}+C_\alpha)\dfrac{r^{-l}-R_c^{-2l}r^l}{1-(b/R_c)^{2l}}, & b<r<R_c,\end{cases} \tag{70}$$

where the subscript $\alpha=1$ and 2 denote the hollow beam 1 and 2, and the constants B_α and C_α can be related by integrating Eqs. (67) and (68) across the discontinuities at $r=a$ and $r=b$. After carrying out a straightforward algebraic manipulation, we obtain the dispersion relation for coupled transverse oscillation,

$$\Gamma_{11}(\omega,k)\cdot\Gamma_{22}(\omega,k)=\Gamma_{12}(\omega,k)\cdot\Gamma_{21}(\omega,k), \tag{71}$$

where the dielectric functions of the hollow beams are defined by

$$\Gamma_{11}=D_1(\omega,k)-\frac{H_1(a)H_2(b)}{4}(1-\beta_1\beta_2)^2\left(1-\frac{b^{2l}}{R_c^{2l}}\right)$$
$$\times\left(1-\frac{a^{2l}}{b^{2l}}\right), \tag{72}$$

$$\Gamma_{22}=D_2(\omega,k)-\frac{H_2(a)H_1(b)}{4}(1-\beta_1\beta_2)^2\left(1-\frac{b^{2l}}{R_c^{2l}}\right)$$
$$\times\left(1-\frac{a^{2l}}{b^{2l}}\right), \tag{73}$$

$$\Gamma_{12}(\omega,k)=\frac{H_2(a)H_1(b)}{4\gamma_1^2}(1-\beta_1\beta_2)\left(1-\frac{a^{2l}}{b^{2l}}\right)\left(1-\frac{b^{2l}}{R_c^{2l}}\right)$$
$$-\gamma_2^2(1-\beta_1\beta_2)[D_2(\omega,k)-1], \tag{74}$$

and

$$\Gamma_{21}(\omega,k)=\frac{H_1(a)H_2(b)}{4\gamma_2^2}(1-\beta_1\beta_2)\left(1-\frac{a^{2l}}{b^{2l}}\right)\left(1-\frac{b^{2l}}{R_c^{2l}}\right)$$
$$-\gamma_1^2(1-\beta_1\beta_2)[D_1(\omega,k)-1]. \tag{75}$$

In Eqs. (72) and (73), $D_\alpha(\omega,k)$ is the diocotron dielectric function, defined by

$$D_\alpha(\omega,k)=1+\frac{H_\alpha(b)}{2\gamma_\alpha^2}\left(1-\frac{b^{2l}}{R_c^{2l}}\right)-\frac{H_\alpha(a)}{2\gamma_\alpha^2}\left[1-\frac{a^{2l}}{R_c^{2l}}\right.$$
$$\left.+\frac{H_\alpha(b)}{2\gamma_\alpha^2}\left(1-\frac{a^{2l}}{b^{2l}}\right)\left(1-\frac{b^{2l}}{R_c^{2l}}\right)\right]. \tag{76}$$

Equation (71) is the dispersion relation of the coupled transverse oscillation, which will be used in the remainder of this section to investigate stability properties for a broad range of system parameters of experimental interest.

In the limit of $n_1\to 0$ or $n_2\to 0$, we recover the dispersion relation of the diocotron instability,[13,14]

$$D_\alpha(\omega,k)=0, \tag{77}$$

for a relativistic hollow electron beam from Eq. (71). It is also instructive to recover the dispersion relation of the regular diocotron instability from Eq. (71), when the two hollow beams have a same velocity of $\beta c=\beta_1 c=\beta_2 c$. In the case of $\beta_1=\beta_2$, the electron density in the dispersion relation is replaced by $n=n_1+n_2$.

This article is copyrighted as indicated in the article. Reuse of AIP content is subject to the terms at: http://scitationnew.aip.org/termsconditions. Downloaded to IP: 35.8.11.3 On: Sun, 24 Jan 2016 23:28:00

B. Stability properties of the coupled transverse oscillation

The stability properties of the coupled transverse oscillations between two hollow electron beams are investigated in this section. As we have seen in the definition $H_\alpha(r)$ in Eq. (69), one of the fundamental quantities in the analysis is the diocotron frequency ω_D of the hollow beam 2, defined by

$$\omega_D=\frac{\omega_{p2}^2}{2\gamma_2^2\omega_c}=\frac{2eI_2}{\gamma_2^2 m\beta_2 c\omega_c(b+a)(b-a)}, \tag{78}$$

which is inversely proportional to the beam thickness $(b-a)$ for a specified beam current I_2. For convenience in the numerical calculation of Eq. (71), we introduce the normalized Doppler-shifted frequency,

$$X=\frac{(\omega-k\beta_2 c)}{\omega_D}, \tag{79}$$

and wave number,

$$\zeta=\frac{kc}{\omega_D}. \tag{80}$$

For relatively short-wavelength perturbations satisfying $|\zeta|\gg 1$, the dispersion relation in Eq. (71) is simplified to

$$D_2(\omega,k)=0, \quad \text{for } |X|\ll|\zeta\,\Delta\beta| \tag{81}$$

and

$$D_1(\omega,k)=0, \quad \text{for } |X+\zeta\,\Delta\beta|\ll|\zeta\,\Delta\beta|. \tag{82}$$

We remind the reader that the dispersion relations in Eqs. (81) and (82) are fundamentally different from the diocotron dispersion relation in Eq. (77), although the apparent forms are similar. The diocotron instability in the dispersion relation in Eq. (77) is based on a rotational shear in one electron fluid element, assuming that $n_1\to 0$ or $n_2\to 0$. Meanwhile, the unstable perturbations from the dispersion relations in Eqs. (81) and (82) originate from two different electron fluid elements, which is the manifestation of $|k\,\Delta\beta\,c|\gg\omega_D$. The physical mechanism of instability in Eqs. (81) and (82) is that one fluid element simply rejects the other fluid element if there is enough velocity difference between two fluid elements. Making use of the normalized Doppler-shifted eigenfrequency in Eq. (79), we calculate the normalized growth rate $X_i=\mathrm{Im}\,X$ and Doppler-shifted real frequency $X_r=\mathrm{Re}\,X$ numerically from Eq. (71) for a broad range of system parameters l, n_1/n_2, β_1, β_2, a/b, b/R_c, and $\zeta=kc/\omega_D$. We emphasize that the normalized growth rate X_i calculated in this section is independent of the parameter ω_{p2}^2/ω_c^2, assuming that the applied magnetic field is strong enough to confine the beam electrons in the radial direction.

One of the most deleterious transverse instabilities of the two hollow electron beams is the kink instability characterized by the azimuthal mode number $l=1$. Although the growth rate of the $l=1$ mode may not necessarily be larger than that of the high mode number ($l>1$), any misalignment of the beams initiates a growing perturbation, kicking the beams sideways from one to the other. In the limit of one beam ($n_1\to 0$ or $n_2\to 0$), the dispersion relation in Eq. (71) is simplified to the conventional diocotron dispersion relation in Eq. (77). We also remind the reader that the stability analysis of the diocotron dispersion relation in Eq. (77) predicts stability for the $l=1$ mode.[13,14] If the dispersion relation in Eq. (71) predicts any unstable perturbation for the $l=1$ mode, this instability is caused by the coupling of two electron beams. In other words, the $l=1$ mode instability is a coupled transverse oscillation of two hollow beams. Shown in Fig. 1 are plots of (a) the normalized growth rate X_i and (b) the Doppler-shifted frequency X_r vs $\zeta=kc/\omega_D$ for $l=1$, $n_1/n_2=0.3$, $\beta_2=0.8$, $\beta_1=0.6$, $a/b=0.9$, and $b/R_c=0.8$. There are two unstable branches, as shown in Fig. 1. The growth rate represented by the solid curve in Fig. 1(a) corresponds to the real frequency plotted by the solid curve in Fig. 1(b). Similarly, the growth rate of the dotted curve corresponds to the real frequency of the dotted curve. The growth rate of instability is a substantial fraction of the diocotron frequency, indicating that the instability due to

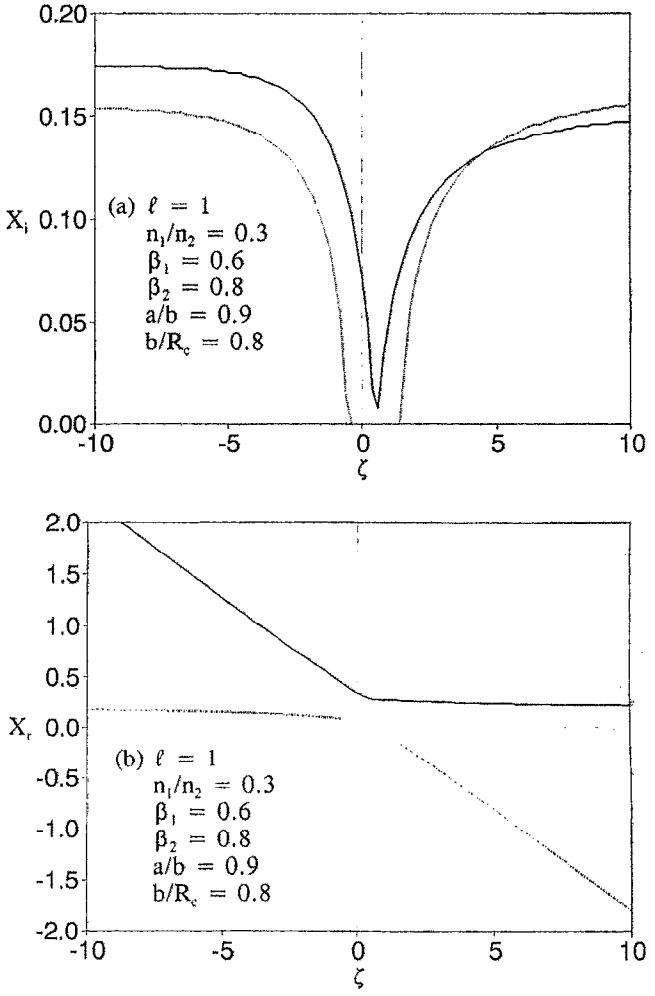

FIG. 1. Plots of (a) normalized growth rate X_i and (b) Doppler-shifted real frequency X_r vs $\zeta=kc/\omega_D$ obtained from Eq. (71) for $l=1$, $n_1/n_2=0.3$, $\beta_2=0.8$, $\beta_1=0.6$, $a/b=0.9$, and $b/R_c=0.8$. Here the Doppler-shifted real frequencies are presented only for the unstable branches.

This article is copyrighted as indicated in the article. Reuse of AIP content is subject to the terms at: http://scitationnew.aip.org/termsconditions. Downloaded to IP: 35.8.11.3 On: Sun, 24 Jan 2016 23:28:00

the coupled transverse oscillation may pose a serious threat to the two-stream klystron without a proper control of the beam misalignment. Assuming that the initial value is Δr, the transverse perturbation $\Delta R(z)$ at the propagation distance z is given by

$$\Delta R(z)=\Delta r \exp\left(\frac{2X_i I_2}{\gamma_2^2\beta_2^2 I_A}\frac{zc}{\omega_c(b^2-a^2)}\right), \tag{83}$$

from Eqs. (78) and (79). In Eq. (83), $I_A=17$ kA is the Alfvén current and $\omega_c=eB_0/mc$ is the nonrelativistic electron cyclotron frequency of the applied magnetic field. As an example, we consider the case of $I_2=5$ kA, the magnetic field $B_0=10$ kG, $\beta_2=0.8$, $b=2.4$ cm, $a/b=0.9$, and the normalized growth rate $X_i=0.15$. The transverse perturbation at the propagation distance z is given by $\Delta r \exp(0.0172z)$ for these parameters. Here, the propagation distance z is in cm unit. Because the two-stream klystron requires a long propagation distance (typically $z>100$ cm) due to a small growth rate of the longitudinal two stream, the initial misalignment Δr must be very small. One way of reducing the growth rate of the coupled transverse oscillation is reduction of the diocotron frequency. As shown in Eq. (78), the diocotron frequency ω_D decreases as the beam thickness increases for specified beam parameters.

When the absolute value of the normalized wave number ζ is much higher than unity, the dispersion relation in Eq. (71) is simplified to Eqs. (81) and (82). For example, the growth rate and real frequency are $X_i=0.155$ and $X_r=0.2$ ($\ll 1$) from Eq. (81), and $X_i=0.169$ and $X_r=2.02\approx\zeta\,\Delta\beta$ from Eq. (82) for $\zeta=-10$ and parameters otherwise identical to Fig. 1. These numbers agree very well with Fig. 1. Figure 2 presents plots of (a) the normalized growth rate X_i and (b) the Doppler-shifted real frequency X_r vs β_1 obtained from Eqs. (71) and (79) for $\zeta=-5$ and parameters otherwise identical to Fig. 1. Obviously, growth rate of the instability in Fig. 2(a) vanishes as the value of the parameter β_1 approaches the value of the parameter β_2. The corresponding Doppler-shifted real frequencies are presented in Fig. 2(b). As predicted in the previous study,[13,14] the $l=1$ mode perturbation is stable when $\beta_1=\beta_2$.

In order to complete the theory of the transverse instability of two hollow electron beams, we analyze the dispersion relation in Eq. (71) for high azimuthal mode numbers. Shown in Fig. 3 are plots of the normalized growth rate X_i versus the parameter β_i obtained from Eq. (71) for $\zeta=0$, several mode numbers l and parameters otherwise identical to Fig. 1. As observed in Fig. 2, growth rate of the $l=1$ mode perturbation decreases to zero as the value of the parameter β_1 approaches that of the parameter β_2. The growth rate of instability for a high azimuthal mode number l decreases slowly as the parameter β_1 approaches the value of the parameter β_2. Dependence of the growth rate of instability on the azimuthal mode number l is illustrated in Fig. 4, where the growth rate X_i is plotted versus the mode number l for $\zeta=0$, $\beta_1=0.6$ and parameters otherwise identical to Fig. 1. The growth rate increases, peaks at $l=9$, and decreases to zero at $l=14$. The growth rate of high azimuthal mode perturbations ($l>1$) is larger than that of the fundamental mode ($l=1$) perturbation. However, as mentioned above, the fundamental mode perturbation is the most deleterious. The high azimuthal mode perturbations will filamentize the beams but have relatively low saturation levels. Filamentation of the beam is tolerable in comparison with the beam deflection due to the kink instability of the $l=1$ perturbation.

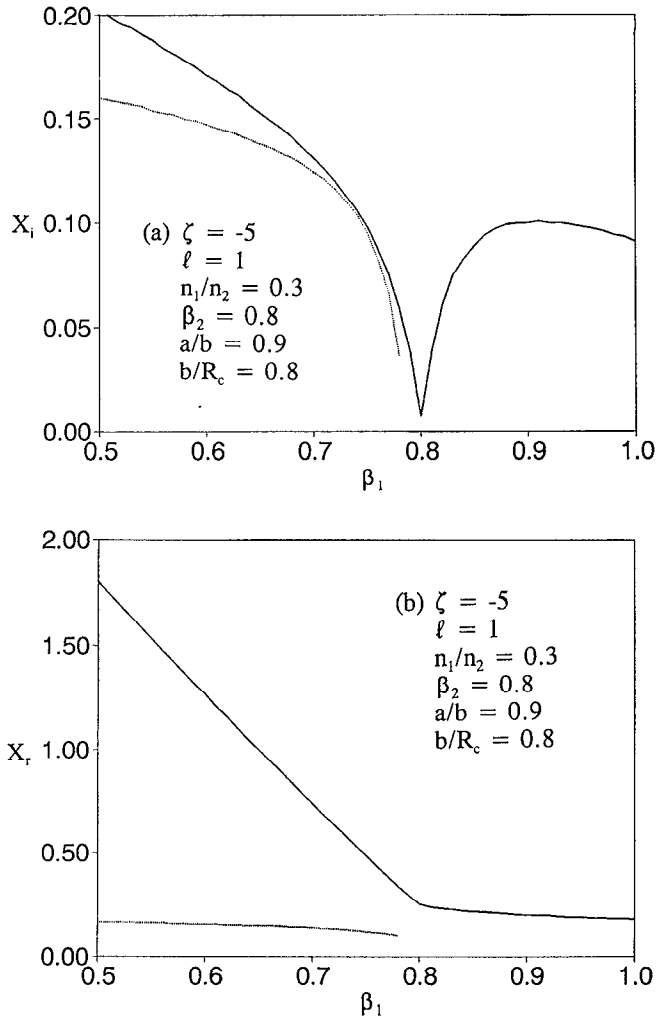

FIG. 2. Plots of (a) normalized growth rate X_i and (b) Doppler-shifted real frequency X_r vs β_1 obtained from Eq. (71) for $\zeta=-5$ and parameters otherwise identical to Fig. 1. Here the Doppler-shifted real frequencies are presented only for the unstable branches.

IV. CONCLUSIONS

Stability properties of two-stream instability of two hollow electron beams were investigated in this paper. The equilibrium configuration consists of two intense relativistic hollow electron beams propagating through a grounded conducting cylinder with radius R_c. The stability analysis of the longitudinal two-stream instability in Sec. II was carried out within the framework of the linearized Vlasov–Maxwell equations for the equilibrium distribution function, in which the beam electrons have same values of the energy and canonical angular momentum, but have a

This article is copyrighted as indicated in the article. Reuse of AIP content is subject to the terms at: http://scitationnew.aip.org/termsconditions. Downloaded to IP: 35.8.11.3 On: Sun, 24 Jan 2016 23:28:00

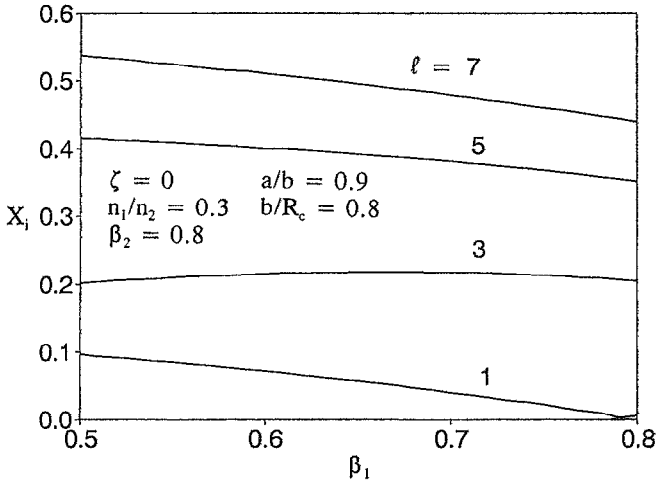

FIG. 3. Plots of normalized growth rate X_i versus parameter β_1 obtained from Eq. (71) for $\zeta=0$, several values of mode number l, and parameters otherwise identical to Fig. 1.

Lorentzian distribution in the axial canonical momentum. The dispersion relation of the longitudinal two-stream instability was obtained, including influence of the axial momentum spread. The stability criterion of the longitudinal two-stream instability derived for the case of zero axial momentum spread indicates that the normalized velocity difference $\Delta\beta$ should be within a certain range of value to be unstable. As shown in an example, even the beams injected from a same cathode can be unstable in an appropriate choice of physical parameters. The growth rate of the longitudinal two-stream instability was analytically calculated for a few limiting cases. The growth rate of instability can be a substantial fraction of the real frequency, thereby indicating that the longitudinal two-stream instability is an effective means of beam current modulation. It

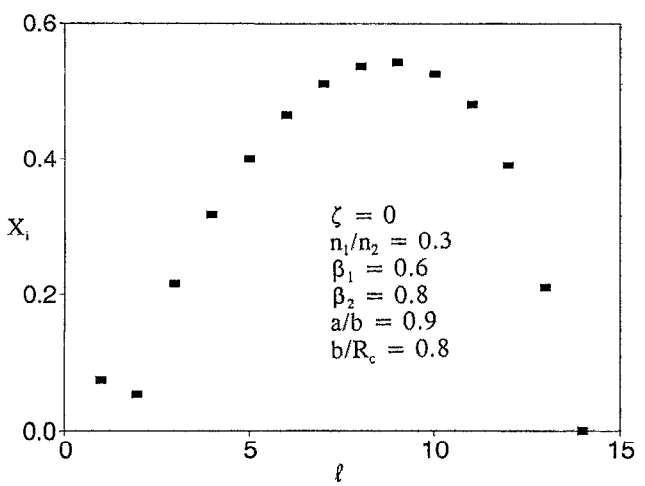

FIG. 4. Plots of normalized growth rate X_i versus the mode number l for $\zeta=0$, $\beta_1=0.6$, and parameters otherwise identical to Fig. 1.

has been also shown that the axial momentum spread stabilizes the longitudinal two-stream instability very effectively.

Transverse instability of hollow electron beams was investigated in Sec. III, assuming that the two beams overlap each other. Dispersion relation for coupled transverse oscillation of two hollow electron beams was derived by making use of the linearized fluid-Maxwell equations. In the limit when one of the beams disappears, the dispersion relation of the coupled transverse oscillation recovers that of the conventional diocotron instability for a hollow electron beam. The dispersion relation of the coupled transverse oscillation was investigated numerically for a broad range of system parameters. It was shown from the numerical calculation of the dispersion relation that the growth rate of the $l=1$ mode instability decreases to zero when the velocity difference $\Delta\beta$ vanishes, as expected. For a large velocity difference between the beams, growth rate of the $l=1$ mode instability is a substantial fraction of the diocotron frequency, thereby indicating that instability due to the coupled transverse oscillation may pose a serious threat to the two-stream klystron, if the beam misalignment is not properly controlled. A numerical investigation of the dispersion relation for a high azimuthal mode number was also carried out.

ACKNOWLEDGMENTS

The author gratefully acknowledges useful discussions with Dr. C. Chen and Dr. M. Friedman.

This research was supported by the Office of Innovative Science and Technology, the Strategic Defense Initiative Organization, managed by the Harry Diamond Laboratories. This work is also supported in part by the Independent Research Fund at the Naval Surface Warfare Center.

[1]M. Friedman, J. Krall, Y. Y. Lau, and V. Serlin, J. Appl. Phys. **64**, 3353 (1988) and the references therein.
[2]Y. Y. Lau, M. Friedman, J. Krall, and V. Serlin, IEEE Trans. Plasma Sci. **PS-18**, 553 (1990), and references therein.
[3]M. Friedman, V. Serlin, A. Drobot, and A. Mondelli, IEEE Trans. Plasma Sci. **PS-14**, 201 (1986).
[4]M. Friedman, J. Krall, Y. Y. Lau, and V. Serlin, Rev. Sci. Instrum. **61**, 171 (1990).
[5]H. S. Uhm, Phys. Fluids B **5**, 190 (1993).
[6]H. S. Uhm, "Enhancement of current modulation in relativistic klystron amplifier," *Engineering Problems and Solutions Workshop on Intense Microwave and Particle Beams*, Los Angeles, CA, 20–24 January, 1992, Technical Program of OE LASE'92 (Society of Photo-optical and Instrumentation Engineers, Los Angeles, CA, 1992), p. 46.
[7]C. Chen, P. Catravas, and G. Bekefi, Appl. Phys. Lett. **62**, 1579 (1993).
[8]J. R. Pierce and W. B. Hebenstreit, Bell Syst. Technol. J. **28**, 33 (1948).
[9]J. R. Pierce, J. Appl. Phys. **20**, 1960 (1949).
[10]A. V. Hollenberg, Bell Syst. Technol. J. **28**, 52 (1948).
[11]A. V. Haeff, Proc. IRE **37**, 4 (1949).
[12]V. Serlin and M. Friedman, Appl. Phys. Lett. **62**, 2772 (1993).
[13]H. S. Uhm and J. G. Siambis, Phys. Fluids **22**, 2377 (1979), and references therein.
[14]R. C. Davidson, *Physics of Nonneutral Plasma* (Addison-Wesley, Reading, MA, 1990), Chap. 6.
[15]H. S. Uhm and R. C. Davidson, Phys. Fluids **24**, 1541 (1981), and references therein.
[16]H. S. Uhm, J. Appl. Phys. **56**, 2041 (1984).
[17]N. A. Krall and A. W. Trivelpiece, *Principle of Plasma Physics* (McGraw-Hill, New York, 1973), Chap. 9.

This article is copyrighted as indicated in the article. Reuse of AIP content is subject to the terms at: http://scitationnew.aip.org/termsconditions. Downloaded to IP: 35.8.11.3 On: Sun, 24 Jan 2016 23:28:00